Mansoura Engineering Journal

Volume 31 | Issue 1 Article 17

12-12-2020

Beam Propagation Method Based on Fast Fourier Transform and Finite Difference Schemes and its Application to Optical Diffraction Grating.

Ahmed Samra
Department of Electronics and Communication Engineering., Faculty of Engineering ., Mansoura University., Mansoura., Egypt

Bedeer Yousif
Electronics and Communications Dept. Faculty of Engineering ., Mansoura University., Mansoura., Egypt

BEAM PROPAGATION METHOD BASED ON FAST FOURIER TRANSFORM AND FINITE DIFFERENCE SCHEMES AND ITS APPLICATION TO OPTICAL DIFFRACTION GRATING

طريقة الإنتشار للشعاع الضوئى المعتمدة على تحويلات فوريير السريعة وطريقة الفروق المحدودة وتطبيقاتها على محزوز الحيود الضوئى

Assoc. prof. Ahmed Shaban Samra
Associate. prof. Faculty of Engineering Mansoura University
Engineer. Bedeer Bedeer Yousif
Electronics and Communications Dept. Faculty of Engineering Mansoura University

ملخص البحث:-

النمذجة الدقيقة للنبائط الفوتونية يعتبر أساس لتطوير المكونات البصرية الجديدة ذات الأداء العالى المطلوبة حاليا ومستقبلا لأنظمة الإتصالات ذى النطاق العريض.
فى هذا البحث نقدم تقنيات متنوعة لهذه النمذجة التى يستخدم العديد منها فى أدوات التصميم التجارية. كما يتضمن هذا البحث تقنيات متنوعة لطرق الإنتشار للشعاع الضوئى مثل تحويلات الفوريير السريعة وطريقة الفروق المحدودة عندما يكون الضوء كمية قياسية و إتجاهية.
وقد تم عمل محاكاه رقميه لمحزوز حيود ضوئى مصنع بتقنية التبادل الأيوني المزدوج كما تم توضيح شكل الإنتشار للمجال الكهربى وحساب زمن البرنامج المستغرق فى كل حاله و قد تم توضيح ذلك بالرسم.
وأوضحت النتائج أن زمن طريقة الفروق المحدودة أصغر من تحويلات الفوريير السريعة بمقدار ٦٦ %.

Abstract—Accurate modeling of photonic devices is essential for the development of new higher performance optical components required by current and future large or wide bandwidth communication systems. This paper introduces several key techniques for such modeling, many of which are used in commercial design tools. These include several techniques of the beam propagation methods (BPM), such as fast Fourier transform (FFT-BPM), wide angle fast Fourier transform (WAFFT-BPM), scalar finite difference (FD-BPM), scalar wide angle finite difference beam propagation method (WAFD-BPM), Generalized Douglas finite difference (GDFD-BPM), and full vectorial finite difference beam propagation method (FVFD-BPM). The numerical simulations are applied to a real optical diffraction grating fabricated by a double–ion exchange technique.

Key words —Beam propagation method (BPM), fast Fourier transform (FFT-BPM), the finite-difference (FD-BPM) and full vectorial finite-difference beam propagation method (FVFD-BPM).

I. INTRODUCTION

THE accurate analysis, design and optimization of guided-wave structures are essential for the development of integrated photonic devices. Of all the methods used to simulate guided-wave propagation in these devices, the beam propagation method (BPM) has been one of the most popular approaches used in the modeling and simulation of electromagnetic wave propagation in guided-wave optoelectronic and fiber-optic devices [1-3]. In this paper, some of the important BPM methods will be discussed. A decided shortcoming of the various conventional beam propagation methods is that they only solve the scalar wave equations under paraxial approximation and hence apply only to simulation of scalar wave propagation along waveguide axis in weakly guiding structures [4-

Accepted March 30, 2006

8]. Several numerical algorithms to treat the vectorial wave propagation have been reported recently [9-11]. The VBPM's are capable of simulating polarized or even hybrid wave propagation in strongly guiding structures. One of the shortcomings of the current VBPM's is that the paraxial approximation is still assumed in the governing equations and only waves propagating close to the waveguide axis may be accurately predicted. In the strongly guided structures, guided modes may be formed by bouncing waves propagating at large angles with the waveguide axis. Even for weakly guided structures, radiation caused by longitudinal index perturbations may occur at large angles of the waveguide axis. Furthermore, a reference refractive index must be assumed in all the paraxial (scalar and vector) propagating algorithms. The choice of the reference index is critical for the accuracy of the numerical solutions. Although an optimum reference index may be obtained by a modal calculation [11], to determine the optimum refractive index in practice is cumbersome and difficult in practical applications.

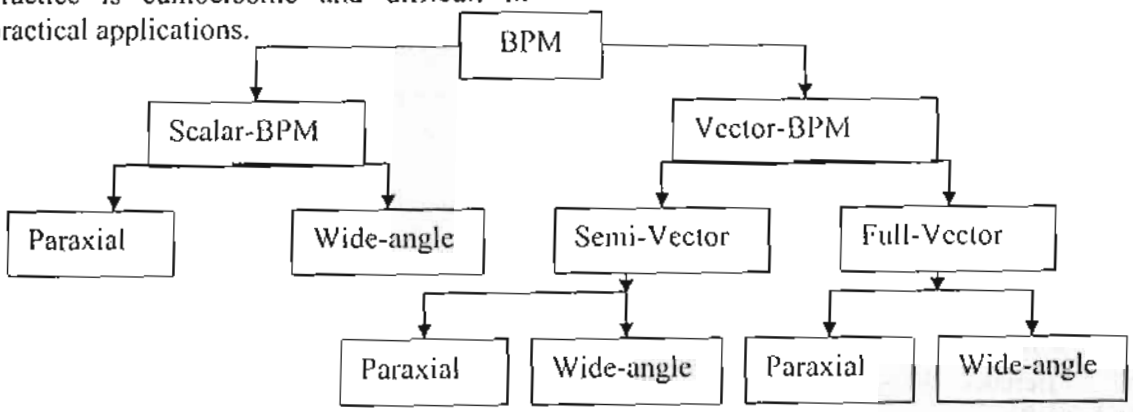

Fig. 1. Different Beam Propagation Methods

The finite-difference (FD) full-vectorial beam propagation method (FVBPM) is widely used for numerical simulation of optical waveguides [12–14]. High numerical accuracy, which is essential for an FVBPM to obtain good stability and convergence behavior for structure modes computation, strongly relies on the specific FD formulas used.

II. BEAM PROPAGATION METHOD CONCEPTS

A. Overview

In this section the concept and capabilities of the beam propagation method (BPM)[1-8] are reviewed. The BPM is the most widely used propagation technique for modeling integrated and fiber-optic photonic devices, and most commercial software for such modeling is based on it. There are several reasons for the popularity of BPM; perhaps the most significant being that it is conceptually straightforward, allowing rapid implementation of the basic technique. This conceptual simplicity also benefits the user of a BPM-based modeling tool as well as the implementer, since an understanding of the results and proper usage of the tool can be readily grasped by a nonexpert in numerical methods. In addition to its relative simplicity, the BPM is generally a very efficient method and has the characteristic that its computational complexity can, in most cases, be optimal, that is to say, the computational effort is directly proportional to the number of grid points used in the numerical simulation. Another characteristic of BPM is that the approach is readily applied to complex geometries without having to develop specialized versions of the method. Furthermore, the approach automatically includes the effects of both guided and radiating fields as well as mode coupling and conversion. Last, the BPM technique is very flexible and extensible,

allowing inclusion of most effects of interest (e.g., polarization, nonlinearities) by extensions of the basic method that fit within the same overall framework [15].

A beam propagation method (BPM) is, as its name suggests, a method used to simulate the propagation of an optical beam excitation along a waveguiding structure. Various kinds of BPMs, such as fast Fourier transformation (FFT-BPM) [1-2] and the finite difference (FD-BPM) [3-14] have been developed. The FFT-BPM and FD-BPM will be discussed here because the original method uses (FFT-BPM) [1-2] whereas the more recent finite difference BPM (FD-BPM) is found to be more efficient and stable when compared to the FFT-BPM [7-8].

A basic assumption of the BPM methods is that the index variation in the propagation direction is small and so may be neglected in the analysis. This effectively eliminates reflected waves from the formulation. This approximation gives two coupled equations for the transverse field components of the propagating wave. The E-formulation, transverse electric field (TE) and M-formulation transverse magnetic field (TM). BPM is based on frequency domain approach and is divided into two parts according to the wave equation (polarization), the first is the Scalar BPM (no polarization), and the second is the Vector BPM (polarization). Each part is divided into two subsections according to the angle of plane waves travelling in the propagation direction, the paraxial (small angle, Parabolic, or Fresnel) and wide angle (Elliptic) for Scalar BPM and vector BPM. Also vector BPM is divided into two sub items according to the coupling terms modes. When ignoring the coupling terms the Vector BPM is called semi vectorial BPM but when consider it the Vector BPM is called full vectorial BPM as shown in Fig (1).

B- Paraxial Scalar BPM

The BPM is essentially a particular approach for approximating the exact wave equation for monochromatic waves, and solving the resulting equations numerically. In this section, the basic approach is illustrated by formulating the problem under the restrictions of a scalar field (i.e., neglecting polarization effects) and paraxiality (i.e., propagation restricted to a narrow range of angles). Subsequent sections will describe how these limitations may be removed. BPM) is based on Maxwell's equations [15] and the scalar wave equation for the propagating beam problem is deduced as [16]

$$\frac{\partial^2 u}{\partial z^2} + 2i\beta\frac{\partial u}{\partial z} + \frac{\partial^2 u}{\partial x^2} + \frac{\partial^2 u}{\partial y^2} + (k^2 - \beta^2)u = 0, \qquad (1)$$

where $k^2 = k_0^2 n^2$, $\beta^2 = k_0^2 n_o^2$ and k is known as the wave- number. In free space, $k_0 = 2\pi/\lambda$. n(x,y) is the refractive index distribution of waveguide structure, and n_o the reference refractive index to be appropriately chosen.

At this point, the above equation is completely equivalent to the exact Helmholtz equation [17]. except that it is expressed in terms of u. It is now assumed that the variation of u with z is sufficiently slow so that the first term of u above can be neglected with respect to the second; this is the familiar slowly varying envelope approximation, and in this context it is also referred to as the paraxial or parabolic approximation. With this assumption and after slight rearrangement, the equation (1) reduces to

$$\frac{\partial u}{\partial z} = \frac{i}{2\beta}\left(\frac{\partial^2 u}{\partial x^2} + \frac{\partial^2 u}{\partial y^2} + (k^2 - \beta^2)u\right) \qquad (2)$$

This is the basic BPM equation in three dimensions (3-D). Simplification to two dimensions (2-D) is obtained by omitting any dependence on y. Given an input field u (x,y,z=0), the above equation determines the evolution of the field in the space $z > 0$. It is important to recognize what has been gained and lost in the above approach. First, the factoring of the rapid phase variation allows the slowly varying field to be represented numerically on a longitudinal grid (i.e., along z) that can be much coarser than the wavelength

for many problems, contributing in part to the efficiency of the technique. Second, the elimination of the second derivative term in z reduces the problem from a second-order boundary value problem requiring iteration or eigenvalue analysis, to a first-order initial value problem that can be solved by simple "integration" of the above equation along the propagation direction. This latter point is also a major factor in determining the efficiency of BPM, implying a time reduction by a factor of at least of the order of (the number of longitudinal grid points) compared to full numerical solution of the Helmholtz equation. The above benefits have not come without a price. The slowly varying envelope approximation limits consideration to fields that propagate primarily along the axis (i.e., paraxiality) and also places restrictions on the index contrast (more precisely, the rate of change of index with z, which is a combination of index contrast and propagation angle). In addition, fields that have a complicated superposition of phase variation, such those existing in multimode devices such as multimode-interference (MMI's), may not be accurately modeled if the phase variation is critical to device behavior. A second key issue beyond the above restrictions on the variation of u is that the elimination of the second derivative also eliminates the possibility for backward traveling wave solutions; thus devices for which reflection is significant will not be accurately modeled. In the following section the numerical solution of the basic BPM equation discussed above is considered.

B-1- Numerical Solutions and Boundary Conditions

Equation (2) is a parabolic partial differential equation that can be "integrated" forward in z by a number of standard numerical techniques. Most early BPM's employed a technique known as the split-step Fourier method [1]. Later work demonstrated that for most problems of interest in integrated optics, an implicit finite-difference approach based on the well-known Crank–Nicholson (CN)scheme was superior [4–8]. This approach and its derivatives have become the standard; thus it is adopted here. It is frequently denoted FD-BPM in the literature, but will be referred to in the following as simply BPM. To create a practical solver we also have to consider the effects of the simulation boundaries on the simulation accuracy. Basic BPM and Mode Solver boundary conditions set the field just outside the simulation area to zero, simulating a perfectly conducting metal box. The energy arriving at the boundaries can be absorbed or otherwise removed to avoid reflected light interfering with the simulation. The popular method is considered in this work, the Transparent Boundary Condition [18-22].

The numerical simulations are applied to diffraction planar grating waveguide [23] as shown in Fig. (2). the measured values of the grating of the effective refractive index of the guided wave mode(n_{e1} and n_{e2}) have done with a He-Ne laser (λ =0.6328) through prism couplers are equal to n_{e1} = 1.512689, n_{e2} = 1.513739 the periodicity of the grating is ($\wedge = 10\ \mu$m) and the incident angle of the optical wavelength as a Bragg angle which is given by

$$\theta_B = \sin^{-1}\left[\frac{\lambda}{2n_{e1}\wedge}\right] \quad \theta_B(\lambda_1) = 1.1985085^{\circ}.$$

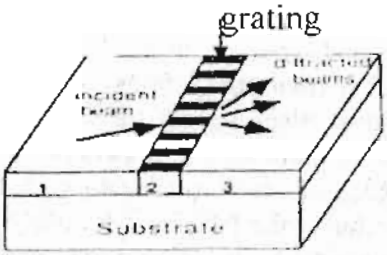

Figure 2. Phase diffraction grating

A Gaussian profile whose full width at half maximum is w_o=10 μm is used as the initial field profile $\Psi_o(x_i, z_o) = \exp(-x_i^2 / w_o^2)$. The computational window is 150 μm for all the simulations. For all methods the accuracy of the

results depend on the number of grid points N in the transverse, i.e., x direction, and the size of the propagation steps, Δz in the direction of propagation, i.e., in z-direction. In all methods N=128, Δz=1 um and the propagation interaction length is 474 um.

B-1-1 *Numerical Solution using fast Fourier transform (FFT-BPM)*

In the beam propagation method one propagates an input field $u(x,z_0)$ over a small distance Δz to obtain the field at $z_0+\Delta z$, [8],[24-25] which is written as

$$u(x,z_0+\Delta z)=\Psi(x,z_0+\Delta z)\exp(i\Gamma) \qquad (3)$$

The phase correction Γ is given by

$$\Gamma=\frac{k^2-\beta^2}{2\beta}\Delta z, \qquad (4)$$

and is evaluated at $(x,z_0+\Delta z)$. The function Ψ satisfies $2i\beta\Psi_z+\Psi_{xx}=0$ and is propagated by using a FFT as follows. If $\Psi_n(z)$ denotes the discrete Fourier transform (DFT) of $\Psi(x,z)$, we have

$$\Psi(x_i,z)=\frac{1}{N}\sum_{n=-N/2}^{N/2}\Psi_n(z)\exp(-ik_n x_i) \qquad (5)$$

where $k_n=2\Pi n/(N\Delta x)$

$$\Psi_n(z_n+\Delta z)=\Psi_n(z_n)\exp(-i\frac{k_n^2}{2\beta}\Delta z) \qquad (6)$$

where the computational domain in x, say, (a,b) has been discretized into N (a power of 2) equal subdivisions, so that $\Delta x=(b-a)/N$ and x_i=a+i Δ x for i=1,N. Note that, although there are N+1 discrete values $\Psi(x_i,z)$, the DFT is applied to only N of them (say ,i=1,N),and the periodicity of the DFT implies that $\Psi_0=\Psi_N$. In connection with this periodicity, note that built into the typical DFT representation chosen above in the fact that u satisfies periodic boundary conditions. Other choices are possible.

In summary, the basic propagation step in the BPM consists of applying Eqn. (3) and (4), where $\Psi(x,z_0+\Delta z)$ is obtained by

1- performing a FFT on $\Psi(x,z_0)=u(x,z_0)$ to obtain $\Psi_n(z_0)$.

2- Computing $\Psi_n(z_0+\Delta z)$ from Eqn. (6).

3- performing an inverse FFT on $\Psi_n(z_0+\Delta z)$ to obtain $\Psi(x,z_0+\Delta z)$. This the basic step is applied repeatedly to obtain the field at any finite propagation distance. The accuracy of the method of course depends on the smallness of the step size Δz and the grid size Δx as well as on the size of computation domain.

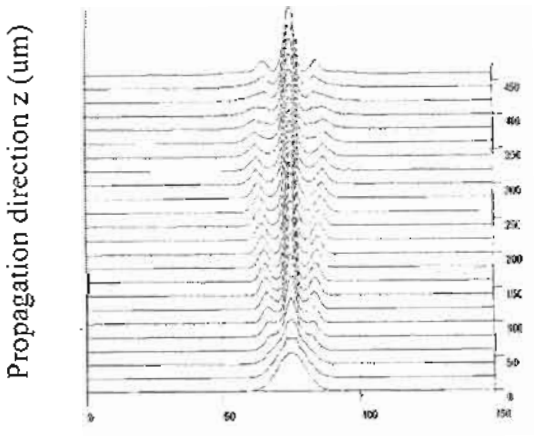

(a) Transverse direction x (μ m)

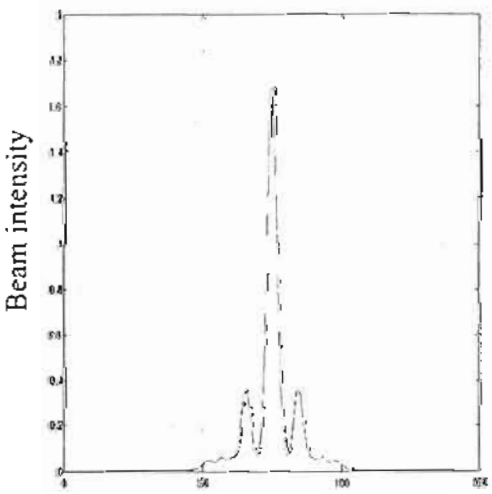

(b) Transverse direction x (μ m)

Fig. (3) A grating BPM solution using FFT
(a) Field profile through 474 μ m of the grating
(b) Output beam intensity of 474 μ m of the grating.

The simulation results are shown in Fig. (3-a,b) for a beam intensity at interaction length 474 μ m. In fig. (3-a) the light propagate in the planar diffraction grating indicates only the zero's and first orders harmonic due to the incident angle of the optical wavelength as a Bragg angle. The simulation result agree with theoretical analysis and the grating device [23] is an excellent integrated optics for light propagation and diffracted.

B-1-2 - *Numerical solution using finite difference (FD-BPM)*

In the finite-difference approach, the field in the transverse (x,y) plane is represented only at discrete points on a grid, and at discrete planes along the longitudinal or propagation direction (z)[7]. Given the discretized field at one plane, the goal is to derive numerical equations that determine the field at the next plane. This elementary propagation step is then repeated to determine the field throughout the structure. For simplicity, the approach is illustrated for a scalar field in 2-D (x,z). Let u_i^n denote the field at transverse grid point i and longitudinal plane n , and assume that the grid points and planes are equally spaced by Δ x and Δ z apart, respectively. In the Crank–Nicholson method (CN), Eqn. (2) is represented at the mid plane between the known plane and the unknown plane as follows:

$$\frac{\partial u}{\partial z} = \frac{i}{2\beta}\left(\frac{\partial^2 u}{\partial x^2} + (k^2 - \beta^2)u\right) \qquad (7)$$

$$\frac{u_i^{n+1} - u_i^n}{\Delta z} =$$

$$\frac{i}{2\beta}\left(\frac{\delta^2}{\Delta x^2} + (k(x_i - z_{n+1/2})^2 - \beta^2)\right)\frac{u_i^{n+1} + u_i^n}{2} \qquad (8)$$

Here δ^2 represents the standard second order difference operat $\delta^2 u_i = u_{i-1} - 2u_i + u_{i+1}$ and $z_{n+1/2} = z_n + \Delta z/2$. The above equation can be rearranged into the form of a standard tridiagonal matrix equation for the unknown field u_i^{n+1} in terms of known quantities, resulting in

$$-au_{i-1}^{n+1} + bu_i^{n+1} - au_{i+1}^{n+1} = au_i^n + cu_i^n + au_i^n \qquad (9)$$

where

$$a = \frac{\Delta z}{2\Delta x^2} \quad , \quad b = \frac{\Delta z}{\Delta x^2} - \frac{\Delta z k_o^2}{2}(n_i(z+\Delta z) - n_o^2) + 2jk_o n_o$$

and $$c = -\frac{\Delta z}{\Delta x^2} + \frac{\Delta z}{2}k_o^2(n_i^2(z) - n_o^2) + 2jk_o n_o$$

These results in a tridiagonal system of linear equations, which can be solved very efficiently [17].

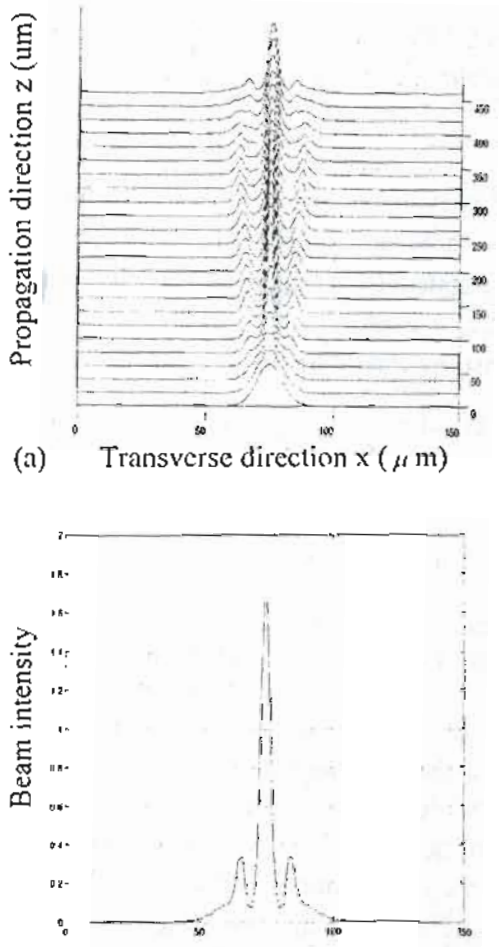

Fig. (4) A grating BPM solution using FD
(a) Field profile through 474 um of the grating
(b) Output beam intensity of 474 um of the grating.

The solution to this system of equations can be also shown to be stable. The simulation results

are shown in fig. (4-a,b) for a beam intensity at interaction length 474 μ m.

B-1-3- *Solution using generalized Douglas finite difference (GDFD-BPM)*

We first summarize the GDFD scheme in a two-dimensional problem [31]. The Fresnel equation for the propagating beam problem is expressed as

$$\frac{\partial u}{\partial z} = \frac{i}{2\beta}\left(\frac{\partial^2 u}{\partial x^2} + (k^2 - \beta^2)u\right) \qquad (10)$$

The philosophy behind the Douglas scheme is to eliminate the truncation error term of the order Δ^2 where Δ is the transverse sampling width. When the truncation error is included, by Taylor's series expansion the second derivative of function u with respect to x is expressed as

$$\frac{\partial^2 u}{\partial x^2} = \frac{\delta^2 u}{\Delta x^2} - \frac{1}{12}\frac{\partial^4 u}{\partial x^4}\Delta x^2 + O(\Delta x)^4 \qquad (11)$$

In the conventional CN scheme, only the first term on the right-hand side of (11) is evaluated, so that the truncation error is $O(\Delta x^2)$.To reduce the truncation error, we substitute (10) into (11) ,replacing $\partial^4 u/\partial x^4$ With $\delta^2(2i\beta\partial u/\partial z - (k^2-\beta^2)u)/\Delta x^2 + O(\Delta x)^2$ Then, the following difference equation can be derived:

$$\frac{\delta^2 u}{\Delta x^2} = \frac{1}{12}(2i\beta\frac{\partial u}{\partial z})_{i+1} + \frac{5}{6}(2i\beta\frac{\partial u}{\partial z})_i + \frac{1}{12}(2i\beta\frac{\partial u}{\partial z})_{i-1} - \frac{1}{12}((k^2-\beta^2)u)_{i+1} - \frac{5}{6}(k^2-\beta^2)u)_i - \frac{1}{12}((k^2-\beta^2)u)_{i-1} + O(\Delta x)^4 \qquad (12)$$

We now introduce the z differencing and get

$$\frac{2i\beta}{12}\frac{u_{i+1}^{l+1}-u_{i+1}^{l}}{\Delta z} + \frac{10i\beta}{6}\frac{u_i^{l+1}-u_i^{l}}{\Delta z} + \frac{2i\beta}{12}\frac{u_{i-1}^{l+1}-u_{i-1}^{l}}{\Delta z} = \frac{(\delta^2 u)_i^{l+1}-u_i^{l}}{2(\Delta x)^2} + \frac{1}{24}[(vu)_{i+1}^{l+1} + (vu)_{i+1}^{l}] + \frac{5}{12}[(vu)_i^{l+1} + (vu)_i^{l}] + \frac{1}{24}[(vu)_{i-1}^{l+1} + (vu)_{i-1}^{l}] + O(\Delta z)^2 + O(\Delta x)^4 \qquad (13)$$

where $v = k_n^2(n^2 - n_n^2)$ .As a result, we obtain the following high accuracy six-point scheme:

$$a_{i-1}^{l+1}u_{i-1}^{l+1} + a_i^{l+1}u_i^{l+1} + a_{i+1}^{l+1}u_{i+1}^{l+1} = a_{i-1}^{l}u_{i-1}^{l} + a_i^{l}u_i^{l} + a_{i+1}^{l}u_{i+1}^{l} \qquad (14)$$

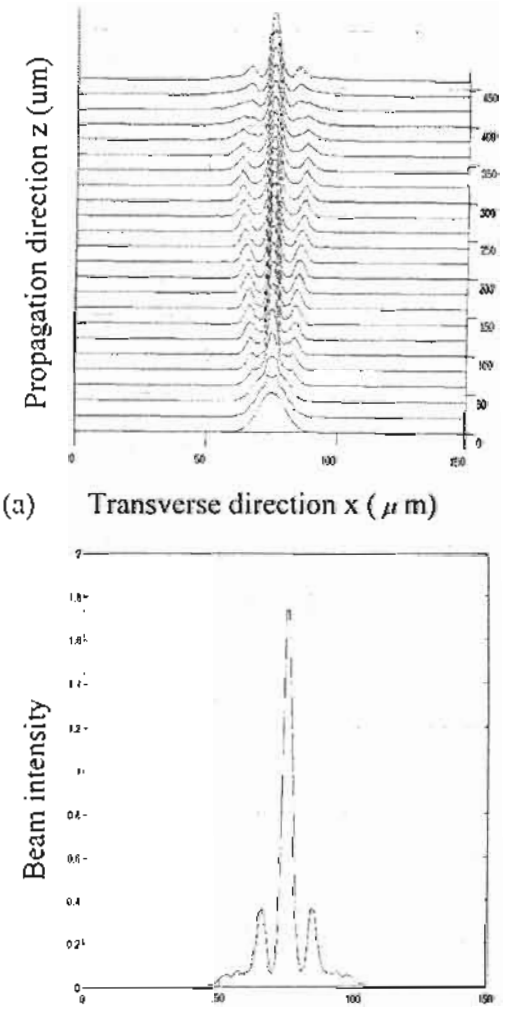

Fig. (5) A grating BPM solution using GDFD (a) Field profile through 474 um of the grating . (b) Output beam intensity of 474 μ m of the grating.

The calculation proceeds as the finite difference method and the simulation results are shown in

fig. (5) for a beam intensity at interaction length 474 um.

C- Scalar Wide Angle *BPM*

The paraxiality restriction on the BPM, as well as the related restrictions on index-contrast and multimode propagation noted earlier, can be relaxed through the use of extensions of BPM that have been referred to as wide-angle BPM [27–31]. The essential idea behind the various approaches is to reduce the paraxial limitations by incorporating the effect of the term that was neglected in the derivation of the basic BPM. The different approaches vary in the method and degree of approximation by which they accomplish this. The most popular formulation is referred to as the multistep Padé-based wide-angle technique [29], [31], and is summarized below.

A simple approach for deriving a wide-angle BPM equation is to consider the Helmholtz wave equation written as [25]

$$[\frac{\partial}{\partial z} - j\beta(1-\sqrt{1+\hat{l}})]\psi(x,y,z) = 0\,, \qquad (15)$$

where $\hat{l} = \dfrac{\dfrac{\partial^2}{\partial x^2} + \dfrac{\partial^2}{\partial y^2} + (k^2 - \beta^2)}{\beta^2}$

C-1- *Numerical solution using wide angle FFT-BPM*

A fast Fourier transform approximation is applied to the z derivative operator in (15) using $\Psi_n(z_o + \Delta z) =$

$$\Psi_n(z_o)\exp[j(\beta - \sqrt{\beta^2 + \frac{\partial^2}{\partial x^2} + \frac{\partial^2}{\partial y^2} + (k^2 - \beta^2)})\Delta z]$$

$$= \Psi_n(z_o)\exp[-j\frac{\Delta z}{2}\frac{\frac{\partial^2}{\partial x^2} + \frac{\partial^2}{\partial y^2}}{(\beta^2 + \frac{\partial^2}{\partial x^2} + \frac{\partial^2}{\partial y^2})^{1/2} + \beta}] \qquad (16)$$

$$\times \exp(-j\frac{(k^2 - \beta^2)\Delta z}{2\beta})\exp[-j\frac{\Delta z}{2}\frac{\frac{\partial^2}{\partial x^2} + \frac{\partial^2}{\partial y^2}}{(\beta^2 + \frac{\partial^2}{\partial x^2} + \frac{\partial^2}{\partial y^2})^{1/2} + \beta}]$$

This is a wide angle formulation , so the operator for the propagation over $\Delta z/2$ in the Fresnel approximation corresponds to that in the wide angle formulation as follows:

$$\exp[-j\frac{\Delta z}{4\beta}\frac{\partial^2}{\partial x^2} + \frac{\partial^2}{\partial y^2}] \leftrightarrow \exp[-j\frac{\Delta z}{2}\frac{\frac{\partial^2}{\partial x^2} + \frac{\partial^2}{\partial y^2}}{(\beta^2 + \frac{\partial^2}{\partial x^2} + \frac{\partial^2}{\partial y^2})^{1/2} + \beta}] \qquad (17)$$

[Fresnel approximation] ↔ [wide angle formulation].

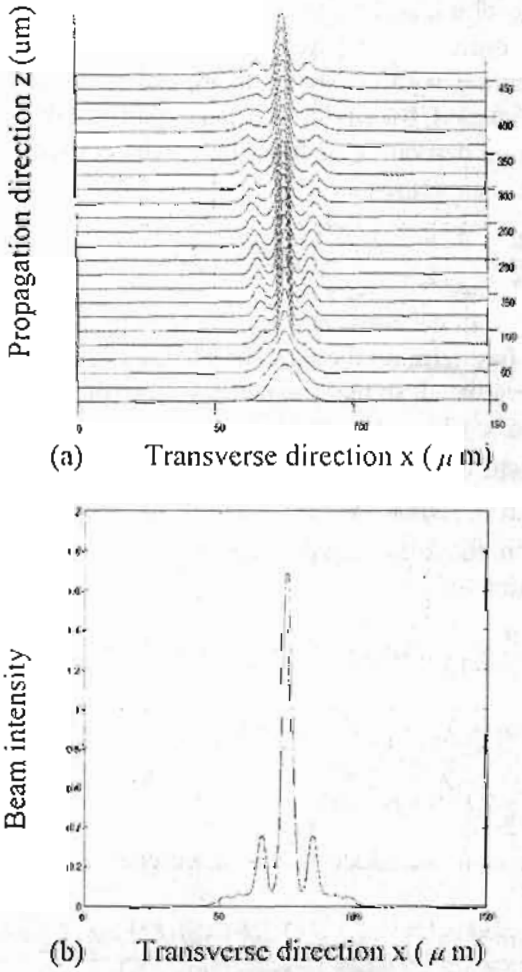

Fig. (6) A grating BPM solution using wide angle FFT

(a)Field profile through 474 μ m of the grating

(b) Output beam intensity of 474 μ m of the grating.

The calculation procedures for the beam propagation based on the wide-angle formulation are exactly the same as those for the beam propagation based on the Fresnel approximation. The simulation results are shown in Fig. (6) for a beam intensity at interaction length 474 μ m.

C-2-Numerical *solution using wide angle FD-BPM*

A finite difference approximation is applied to the z derivative operator in (15) using:

$$[\frac{1}{\Delta z}-\alpha j\beta(1-\sqrt{1+\hat{I}})]\psi(x,y,z+\Delta z)=$$

$$[\frac{1}{\Delta z}+(1-\alpha)j\beta(1-\sqrt{1+\hat{I}})]\psi(x,y,z) \quad (18)$$

The Padé expansion of the square root operator is [32]:

Where $$\sqrt{1+\hat{I}}=1+\sum_{k=1}^{n}\frac{a_{k,n}\hat{I}^{k}}{1+b_{k,n}\hat{I}^{k}}$$

$a_{k,n}=\frac{2}{2n+1}\sin^2(\frac{k\pi}{2n+1})$ and $b_{k,n}=\cos^2(\frac{k\pi}{2n+1})$

Substituting (18) into (15) and Taking the first order Padé expansion and substituting in the coefficients are get the Padé (1,1) wide angle scheme:

$$[4+(1+2\Delta z\alpha j\beta)\hat{I}]\psi(x,y,z+\Delta z)=$$

$$[4+(1-2\Delta z(1-\alpha)j\beta)\hat{I}]\psi(x,y,z) \quad (19)$$

The $\hat{I}$ operator is not raised to a higher power in the Padé (1, 1) scheme which effectively means that a higher order expansion of $\sqrt{1+\hat{I}}$ is achieved over the paraxial case with negligible extra computational effort. Higher order Padé schemes are derived by further expanding the expressions in equation (18). This leads to higher powers in $\hat{I}$ which if implemented directly would create large bandwidth matrices which are cumbersome to solve. The solution is to express (18) as a product of operators. In summary, the solution of wide-angle scalar equation can be obtained from [28-31].

$$\frac{\partial\psi}{\partial z}=j\beta\frac{N_m(P)}{D_n(P)}\psi \quad (20)$$

where $D=\frac{\partial}{\partial z}$, $p=\hat{I}$. Here N_m and D_n are polynomials in the operator p and (m,n) is the order of the approximation. Table I shows several common approximants. When (20) is employed, larger angles, higher index contrast, and more complex mode interference can be analyzed in both guided wave and free space problems as the Padé order(m,n) is increased [27-29]. Guidelines for using the technique and a discussion of the complex interrelationships between waveguide angle, index contrast, Padé order, reference wave number and grid parameters are discussed in [25],[29]. The simulation results are shown in Fig. (7) for a beam intensity at interaction length 474 μ m.

Padé Order (m,n)	Nm	Dn
(1,0)	P/2	1
(1,1)	P/2	1+P/4
(2,1)	P/2+ P^2/8	1+P/2
(2,2)	P/2+P^2/4	1+3P/4+ P^2/16
(3,2)	P/2+3P^2/8+P^3/32	1+P+ 3P^2/16
(3,3)	P/2+P^2/2+3P^3/32	1+5P/4+ 3P^2/8+P^3/64
(4,3)	P/2+5P^2/8+3P^3/16+P^4/128	1+3P/2+5P^2/8+P^3/16
(4,4)	P/2+3P^2/4+5P^3/16+P^4/32	1+7P/4+15P^2/16+5P^3/32+P^4/256

Table I shows several common Padé approximants

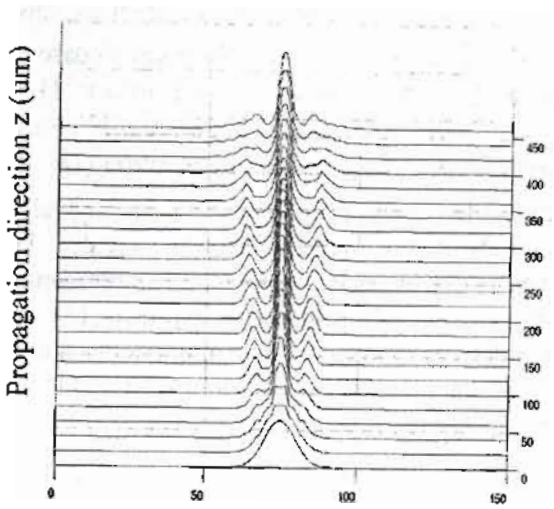

(a) Transverse direction x (μ m)

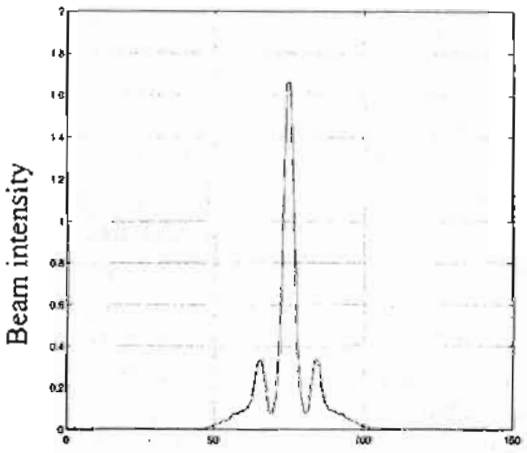

(b) Transverse direction x (μ m)

Fig. (7) A grating BPM solution using wide angle FD (a) Field profile through 474 um of the grating (b) Output beam intensity of 474 μ m of the grating.

D- Paraxial Vector BPM

Polarization effects can be included in the BPM by recognizing that the electric field is a vector, and starting the derivation from the vector wave equation rather than the scalar Helmholtz equation [32-33]. In one approach, the equations are formulated in terms of the transverse components of the field (E_x and E_y), and result in the following set of coupled equations for the corresponding slowly varying fields (u_x and u_y)[34-35]

$$\frac{\partial u_x}{\partial z} = A_{xx}u_x + A_{xy}u_y \qquad (21)$$

$$\frac{\partial u_y}{\partial z} = A_{yx}u_x + A_{yy}u_y \qquad (22)$$

The A_{ij} are complex differential operators given by

$$A_{xx}u_x = \frac{i}{2\beta}\{\frac{\partial}{\partial x}[\frac{1}{n^2}\frac{\partial}{\partial x}(n^2u_x)] + \frac{\partial^2}{\partial y^2}u_x + (k^2-\beta^2)u_x\} \quad (23\text{-a})$$

$$A_{yy}u_y = \frac{i}{2\beta}\{\frac{\partial^2}{\partial x^2}u_y + \frac{\partial}{\partial y}[\frac{1}{n^2}\frac{\partial}{\partial y}(n^2u_y)] + (k^2-\beta^2)u_y\} \quad (23\text{-b})$$

$$A_{yx}u_x = \frac{i}{2\beta}\{\frac{\partial}{\partial y}[\frac{1}{n^2}\frac{\partial}{\partial x}(n^2u_x)] - \frac{\partial^2}{\partial y\partial x}u_x\} \text{ and}$$

$$A_{xy}u_y = \frac{i}{2\beta}\{\frac{\partial}{\partial x}[\frac{1}{n^2}\frac{\partial}{\partial y}(n^2u_y)] - \frac{\partial^2}{\partial x\partial y}u_y\} \quad (23\text{-c})$$

The operators A_{xx} and A_{yy} account for polarization dependence due to different boundary conditions at interfaces and describe such effects as different propagation constants, field shapes, bend loss, etc., for TE and TM fields. The off-diagonal terms involving A_{xy} and A_{yx} account for polarization coupling and hybrid modes due to geometric effects, such as the influence of corners or sloping walls in the cross-sectional structure (effects due to material anisotropy are considered below).

The above equations are generally referred to as describing a full-vectorial BPM. The simplification $A_{xy} = A_{yx} = 0$ gives the important semi-vectorial approximation. In two-dimension analysis, the semi-vectorial approximation is equivalent to the full vectorial. In this case the transverse field components are decoupled, simplifying the problem considerably while retaining what are usually the most significant polarization effects. Unless a structure is specifically designed to induce coupling, the effect of the off-diagonal terms is extremely weak and the semi-vectorial approximation is an excellent one. The numerical method used to solve the vector BPM is the finite difference method but Fourier transform has the following disadvantages [25] due to the nature of FFT: (1) it requires a long computation time, (2) the discretization widths in the lateral directions must be uniform, (3) the simple transparent boundary condition cannot be used at the analysis

boundaries, (4) very discretization widths cannot be used in the lateral directions, (5) the polarization cannot be treated, (6) it is inadequate for large refractive index reference optical waveguides, (7) the number of sampling points must be a power of 2, (8) the propagation step has to be small.

D-1- *Numerical solution using finite difference paraxial vector-BPM*

Equation (22) can be solved by using the finite-difference method. In the finite-difference solutions, the real continuous space is discretized into a lattice structure defined in the computation region. The field at the lattice point of $x = m\Delta x$, $y = n\Delta y$ and $z = l\Delta z$ is represented by $u_x^l(m,n)$. For the transverse derivatives, a central difference scheme is used which attains the second-order accuracy in space. Since is simply given by the transverse derivatives, a central difference scheme is the tangential electric fields are continuous across the index interfaces, the finite-difference approximation for $\partial^2 u_x / \partial y^2$ is simply given by

$$\frac{\partial^2 u_x}{\partial y^2} = \frac{u_x{}^l(m,n+1) - 2u_x{}^l(m,n) + u_x{}^l(m,n-1)}{\Delta y^2} \quad (24)$$

For the derivative along the direction of the polarization, the discontinuities of the normal electric fields across the index interfaces should be considered. The standard central difference can still be applied formally, but the field values at the two adjacent points should be modified according to the boundary conditions across the possible index interfaces between the lattice points. The finite-difference expression for $\partial^2 u_x / \partial x^2$ becomes [36]

$$\frac{\partial^2 u_x}{\partial x^2} = T^l{}_{m+1,n} u_x{}^l(m+1,n)/(\Delta x)^2 - \quad (25)$$

$$[2 - R^l{}_{m+1,n} - R^l{}_{m-1,n}] u_x{}^l(m,n)/(\Delta x)^2 +$$

$$T^l{}_{m-1,n} u_x{}^l(m,n-1)/(\Delta x)^2,$$

where $T^l{}_{m\pm1,n} = \dfrac{2n^2(m\pm1,n,l)}{n^2(m\pm1,n,l) + n^2(m,n,l)}$,

$$T^l{}_{m\pm1,n} = \frac{2n^2(m\pm1,n,l)}{n^2(m\pm1,n,l) + n^2(m,n,l)}, \quad (26)$$

Making use of (30) and (31), we derive the following finite-difference equations

$$A^{l+1}_{m,n} u^{l+1}_{x(m,n)} + A^{l+1}_{m+1,n} u^{l+1}_{x(m+1,n)} + A^{l+1}_{m-1,n} u^{l+1}_{x(m-1,n)} +$$
$$A^{l+1}_{m,n+1} u^{l+1}_{x(m,n+1)} + A^{l+1}_{m,n-1} u^{l+1}_{x(m,n-1)} = \quad (27)$$
$$A^{l}_{m,n} u^{l}_{x(m,n)} + A^{l}_{m+1,n} u^{l}_{x(m+1,n)} + A^{l}_{m-1,n} u^{l}_{x(m-1,n)} +$$
$$A^{l}_{m,n+1} u^{l}_{x(m,n+1)} + A^{l}_{m,n-1} u^{l}_{x(m,n-1)}$$

where $A^{l+1}_{m,n} = 1 - j\dfrac{\alpha\Delta z}{2\beta}\{\dfrac{1}{(\Delta x)^2}[2 - R^{l+1}_{m+1,n} - R^{l+1}_{m-1,n}] +$

$$\frac{2}{(\Delta y)^2} - [n^2{}_{m,n,l+1} - n_o^2]k_o^2\} \quad (28\text{-a})$$

$$A^{l+1}_{m\pm1,n} = j\frac{\alpha T^{l+1}_{m\pm1,n}\Delta z}{2\beta(\Delta x)^2}, \quad A^{l+1}_{m,n\pm1} = j\frac{\alpha\Delta z}{2\beta(\Delta y)^2} \quad (28\text{-b})$$

$$A^{l}_{m,n} = 1 + j\frac{(1-\alpha)\Delta z}{2\beta}\{\frac{1}{(\Delta x)^2}[2 - R^{l}_{m+1,n} - R^{l}_{m-1,n}] +$$

$$\frac{2}{(\Delta y)^2} - [n^2{}_{m,n,l} - n_o^2]k_o^2\} \quad (28\text{-c})$$

$$A^{l}_{m\pm1,n} = -j\frac{(1-\alpha)T^{l}_{m\pm1,n}\Delta z}{2\beta(\Delta x)^2}, \quad (28\text{-d})$$

$$A^{l}_{m,n\pm1} = -j\frac{(1-\alpha)\Delta z}{2\beta(\Delta y)^2}$$

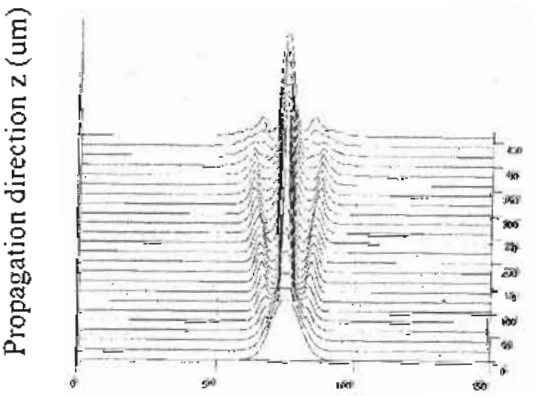

(a) Transverse direction x (μ m)

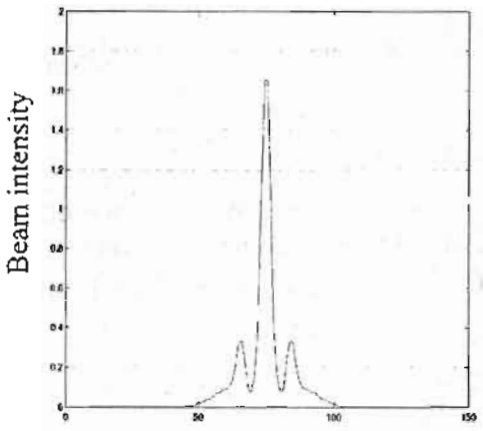

(b) Transverse direction x (μ m)

Fig. (8) A grating BPM solution using paraxial FVFD (a) Field profile through 474 μ m of the grating (b) Output beam intensity of 474 μ m of the grating.

The parameter α is introduced to control the finite-difference scheme. For instance, $\alpha = 0.5$ corresponds to the Crank-Nicholson scheme. The choice of α may affect the stability, the order of accuracy, and the numerical dissipation and dispersion of the FD-VBPM [31-32]. It can be proved that the finite-difference scheme in (27) and (28) is unconditionally stable for $\alpha \geq 0.5$. Equation (27) may be solved numerically at each propagating step. For the 2-D problems, following a standard lower upper decomposition (LUD) for the tridiagonal linear equations can be used. For the 3-D problem, we can apply the ORTHOMIN method [37]. The simulation results are shown in fig. (8) for a beam intensity at interaction length 474 μ m.

E- *Numerical solution using a wide angle vector-BPM*

By utilizing the Padé recursion relation [38]

$$\frac{\partial}{\partial z}\Big|_{n+1} = \frac{-jA_n}{1 + j\frac{1}{2\beta}\frac{\partial}{\partial z}\Big|_n}$$ where i=x, y wide

angle schemes of different orders may be derived for 2D from (21) for n=1, the following equation is obtained:

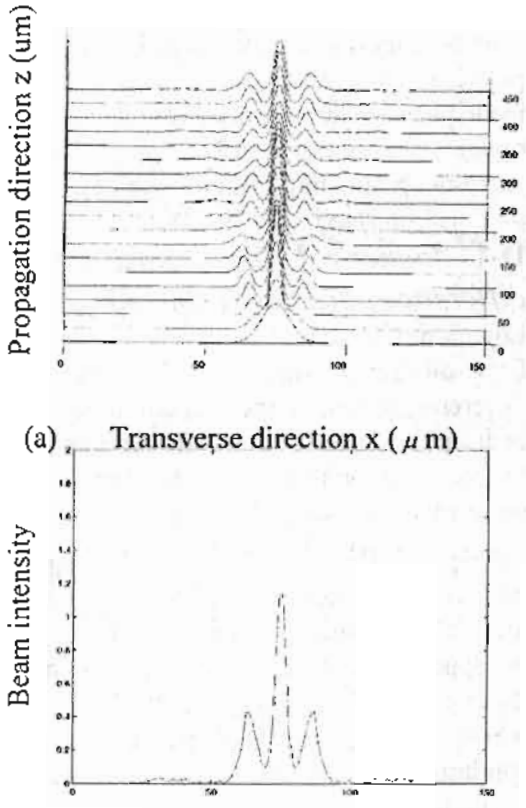

(b) Transverse direction x (μ m)

Fig. (9) A grating BPM solution using wide-angle FVFD (a) Field profile through 474 μ m of the grating (b) Output beam intensity of 474 μ m of the grating.

$$[1 + \frac{A_n}{2\beta} - j\Delta z\alpha A_n]u_i^{n+1} = [1 + \frac{A_n}{2\beta} - j\Delta z(1-\alpha)A_n]u_i^n \quad (29)$$

Note that virtually no extra computation is required for the wide angle scheme in comparison with the paraxial VBPM. The simulation results are shown in fig. (9) for a beam intensity at interaction length 474 μ m

F- Accuracy of BPMs

To assess the accuracy we calculated the beam intensity at interaction length 474 um as a function of the grid points in the transverse direction X and step propagation Δ z in z direction. These results are shown in previous Figures. For all methods as N gets larger and Δ z gets smaller, accuracy improves. For the slowly varying index case, the accuracy of all methods is not very sensitive to the actual N

value as long as it is not too small. As Δz increases, however, accuracy degrades for all methods . Accuracy of the FFT-BPM starts to degrade at smaller Δz values compared to FD-BPMs . Again as Δz increases accuracy of all methods degrades. Degradation in the FD-BPM result is slower than FFT-BPM.

As another test on the accuracy, we calculated the CPU time for all methods, and the result shown in Fig. (10). Although it is possible to get the same accuracy using all methods, due to the need for a small propagating step, the required computation time effort for FFT-BPM can be drastically higher than that of FD-BPM. To compare the computational speed of all methods we compared the CPU time required for the light propagation through a distance 474 um at N=128 in different BPMs. This is the time it takes to find the field profile away from a known field profile and is independent of the structure under consideration. The number of grid points increases, CPU time per step for all techniques increases. The increase in FFT-BPM is more rapid and over the N values considered FD-BPM is 4 to 6 times faster than FFT BPM.

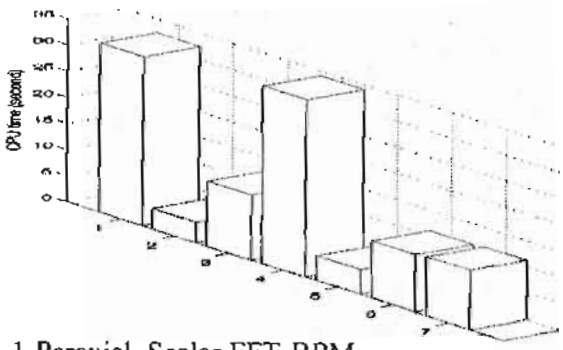

1-Paraxial, Scalar FFT-BPM,
2- Paraxial, Scalar FD-BPM ,
3- Paraxial, Scalar GDFD-BPM,
4- Wide angle scalar FFT-BPM ,
5- Wide angle Scalar FD-BPM,
6-Paraxial, Full vector FD-BPM ,
7-Wide angle Full vector FD-BPM

Fig. (10) CPU time for the different simulation methods.

This is a direct indication of the fact that computation time required to solve a tridiagonal system of N linear equations increases as N, whereas time required to obtain the FFT of a function using N grid points increases as N log N. Comparison of the accuracy of both methods shows that one can get accurate results with larger propagating step sizes in FD-BPM. Combined with the CPU time improvement per step, this indicates that FD-BPM can be much more efficient than FFT-BPM. The computer used in running a program 2.4/512 GHz and 256 MB

IV. CONCLUSIONS

In this paper, a beam propagation method employing a finite difference approximation is studied in comparison with that using fast Fourier transformation. From the study, it is found that the computation time for the simulation in FD-BPM is 66% times less than that of FFT-BPM.

Furthermore, FD BPM is much more stable with respect to propagation step size, Δz, and number of grid points N variations. For comparable accuracy, one needs much smaller propagation step sizes in the FFT-BPM than the FD-BPM. This indicates that combined with the CPU time improvement per step FDBPM can be much more efficient than FFT-BPM. As further test on the accuracy of all methods, From previous analysis we can conclude that our optical diffraction grating fabricated by a double-ion exchange technique is more efficient as an optical waveguide diffraction device and proved to have many applications in optics.

[1] M. D. Feit and J. A. Fleck, Jr. "Light propagation in graded-index optical fibers,"Appl. *Opt.*, vol. 17, no. 24, pp. 3990-3998, 1978.

[2] M.D.Feit and J. A. Fleck, Jr., "Computation of mode properties in optical fiber waveguides by a propagating beam method," Appl. Opr., vol. 19, pp. 1154-1163, 1980.

[3] A. Neyer, W. Mevenkamp, L. Thylen and B. Lagerstrom, "A beam propagation method analysis of active and passive waveguide crossings,"IEEEJ. Lightwave Technol., vol. 3, pp. 635-642, Mar. 1985.

[4] D. Yevick and B. Hermansson, "Efficient beam propagation techniques," IEEE Quantum Electron., vol. 26, pp. 109-112, Jan. 1990.

[5] B. Hermansson, D. Yevick, W. Bardyszewski, and M. Glasn "The unitary of split-operator finite difference and finite-element methods: Applications to longitudinally varying semiconductor rib waveguides," IEEE J. Lightwave Techn., vol. 8, pp.1866-1873, Dec. 1990.

[6] Y. Chung and N. Dagli, "Explicit finite difference beam propagation method Application to semiconductor rib waveguide Y-junction analysis," Elec. Lett., vol. 26, no. 11, pp. 711-713, 1990.

[7] Y. Chung and N. Dagli, "An assessment of finite difference beam propagation method," IEEEJ. Quantum Electron, vol. 26, pp. 1335-1339, Aug. 1990.

[8] R. Scarmozzino and R. M. Osgood, Jr., "Comparison of finite difference and Fourier transform solutions of the parabolic wave equation with emphasis on integrated-optics applications," J. Opt. Soc. Amer. A, vol. 8, no. 5, pp. 727-731, 1991.

[9]W. P. Huang, C. L. Xu, and S. K. Chaudhuri, "A finite-difference vector beam propagation method for three dimensional waveguide structures," *IEEE Photon. Technol. Lett.*, vol. 4, pp. 148-151, Feb. 1992.

[10]Y. Chung, N. Dagli, and L. Thylen, "Explicit finite difference vectorial beam propagation method," *Electron. Lett.*, vol. 37, no. 23, pp. 2119-2121, 1991.

[11] W. P. Huang, C. L. Xu, S. T. Chu, and S. K. Chaudhuri, "The finite difference vector beam propagation method: Analysis and assessment," J.*Lightwave Tech.*, vol. 10, pp. 295-304, Mar. 1992.

[12] W. P. Huang and C. L. Xu, Simulation of three-dimensional optical waveguides by a full-vector beam propagation method *IEEE J. Quan. Elec.*, vol. 29, pp. 2639–2649, Oct. 1993.

[13] Y. L. Hsueh, M. C. Yang, and H. C. Chang, "Three-dimensional noniterative full-vectorial beam propagation method based on the alternating direction implicit method," *J. Lightwave Technol.*, vol. 17, pp. 2389–2397, Nov. 1999.

[14]L. D. S. Alcantara, F. L. Teixeira''A New Full- Vectorial FD-BPM Scheme: Application to the analysis of Magnetooptic and Nonlinear Saturable Media,'' J.*Lightwave Tech.*, vol. 23,No.8 pp. 2579-2585, Aug.2005.

[15] M. Born and E. Wolf, "Principles of Optics", Pergamon Press New York, 1993.

[16] R. Scarmozzino, A. Gopinath, R. Pregla ,and S. Helfert "Numerical Techniques for Modeling Guided-Wave Photonic Devices " IEEE J. *Quan. Elect.* vol. 6, no. 1, Jan. 2000.

[17] J. W. Goodman,' Introduction to Fourier optics', McGraw-Hill Book Company, Inc., 1996

[18] G. R. Hadley, "Transparent Boundary Condition for the Beam Method", IEEE Journal of Quantum Electronics, vol 28, Issue 1, pp 363 – 370, 1992,

[19]C Vassallo and F Collino, "Highly Efficient Absorbing Boundary Conditions for the Beam Propagation Method", Journal of Lightwave Technology, Vol. 14, No. 6, pp. 1570 – 1577,1996.

[20] J. P. Berenger, "A perfectly matched layer for the absorption of electromagnetic waves", J. Comp. Phy., vol. 114, pp. 185-200, , 1994,

[21] W. P. Huang, C L Xu, W. Lui and K. Yokoyama, "The Perfectly Matched Layer (PML) Boundary Condition for the Beam Propagation Method", IEEE Photon. Technol. Lett., Vol. 8, No. 5, pp 649 – 651, 1996.

[22]G. R. Hadley, "Transparent boundary condition for beam propagation, Opt. Lett., vol. 16, no. 9, pp. 624-629, 1991.

[23] Gamma. L, Chartier G.H., Samra. A. S. "A novel technique for making grating demultiplexers in integrated optics ".J. phys. D: Appl. Phys., vol.23, pp.1298-1301,1990,UK

[24] E. o. Brigham,'' The Fast Fourier Transformation''. Englewood Cliffs, NJ; Prentice Hall, , pp. 163-164, 1974

[25] K. Kawano,T. Kitoh," Introduction to optical waveguide analysis",pp.165-231,ch. 5, 2001

[26]J. Yamauchi, J. Shibayama, O. Saito, O. Uchiyama, an H. Nakano," Improved Finite Difference Beam-Propagation Method Based on the Generalized Douglas Scheme and Its Application to Semivectorial Analysis", J. *Lightwave Technol.*, vol.14,pp.2401-2406,Oct.1996.

[27] D. Yevick and M. Glasner, "Analysis of forward wide-angle light propagation in semiconductor rib waveguides and integrated-optic structures," *Electron. Lett.*, vol. 25, pp. 1611–1613, 1989.

[28]G. R. Hadley, "Wide-angle beam propagation using Pade approximant operators," *Opt. Lett.*, vol. 17, p. 1426, 1992.

[29]I. Ilic, R. Scarmozzino, and R. M. Osgood Jr., "Investigation of the Pade approximant-based wide-angle beam propagation method for accurate modeling of waveguiding circuits," *J. Lightwave Technol.*, vol. 14, pp. 2813– 2822, 1996.

[30] G. R. Hadley, "Multistep method for wide-angle beam propagation," *Opt. Lett.*, vol 17, pp. 1743-1744, 1992.

[31]T. Anada, T. Hokazono, T. Hiraoka, J.- P. Hsu, T.M. Benson, P. Sewell, "Very-wide-angle beam propagation methods for integrated optical circuits", IEICE Trans. Electron., vol E82-C, pp. 1154-1158, 1999.

[32] R. Clauberg and P. Von Allmen, "Vectorial beam propagation method for integrated optics," *Electron. Lett.* vol. 27, p. 654, 1991.

[33]M. S. Stern, "Semivectorial polarized finite difference method for optical waveguides with arbitrary index profiles," IEE ***Proc.,*** vol. 135, pt. J., no. 1, pp. 56-63, 1988.

[34] W. P. Huang and C. L. Xu, "Simulation of three-dimensional optical waveguides by a full-vector beam propagation method," *J. Quan. Electron.*, vol. 29, p. 2639, 1993

[35] J. Van Roy, J. van der Donk, and P. E. Lagasse, "Beam propagation method: Analysis and assessment," J. Opt. Soc. Amer., vol. 71, p. 803, 1983.

[36] Y. L. Hsueh, M. C. Yang, and H. C. Chang, "Three-dimensional noniterative full vectorial beam propagation method based on the alternating direction implicit method," *J. Lightwave Technol.*, vol. 17, pp. 2389–2397, Nov. 1999.

[37]Yongzhi He and Frank G.Shi,'' Improved full vectorial beam propagation method with high accuracy for arbitrary optical waveguides",J.photonic *Technol.*, vol. 15, No.10, pp.1381–1383, Oct. 2003.

[38] W.P. Huang and C.L. Xu, "Wide-Angle Vector Beam Propagation Method" J.photonic *Technol.*, vol. 4,No.10, pp. 1118–1120,October 1992.